RESPONSE OF PORTLAND LIMESTONE CEMENT CONCRETE TO HIGH CONCENTRATION OF CHLORIDE-BASED SALTS

Ahmed Ghazy, Research and Standards Engineer, Public Works Department, City of Winnipeg, MB, Canada and Department of Civil Engineering, University of Alexandria, Egypt

Mohamed Bassuoni, Professor, Department of Civil Engineering, University of Manitoba, Winnipeg, MB, Canada

Paper prepared for presentation

at the soils & materials Session

at the 2020 TAC Conference & Exhibition

Abstract: General use limestone (GUL) cement is now permitted in the production of all classes of concrete in Canada. Its contribution to reduction in greenhouse gas emissions and sustainable construction is the main driving force for its development globally. However, there has been dearth of information on the effect of GUL on performance of concrete exposed to high concentration of chloride-based salts. Therefore, the aim of this study is to investigate the response, in terms of physico-mechanical properties and microstructural features, of concrete made with GUL without or with fly ash to highly concentrated chloride solutions (NaCl, $MgCl_2$ and $CaCl_2$). A continuous immersion exposure at 5°C was used to promote formation of complex salts (oxychlorides). The results revealed that GUL mixtures exhibited better resistance to de-icing salts due to synergistic physical and chemical actions of limestone in the cementitious matrix. The resistance of concrete exposed to de-icing salts is a function of physical penetrability (magnitude of intruding solution), amount of aluminate in cement and content of portlandite available for chemical reactions in the hydrated paste. The incorporation of high volume fly ash (30%) had a pronounced effect on improving the concrete resistance to damage as reflected by sound mechanical properties and longevity.

Keywords: General use limestone cement; Fly ash; De-icing salts; Physical and chemical resistances; Oxychlorides.

ACKNOWLEDGEMENTS

INTRODUCTION

General use limestone (GUL) cement, containing up to 15% limestone powder, has been introduced in the Canadian market and is now permitted in the production of all classes of concrete in the latest version of CSA 23.1 (CSA 2019). Its contribution to reduction in greenhouse gas emissions and sustainable construction is the main driving force for its development globally. Reducing the clinker content of cement by up to 15% will effectively reduce the CO_2 emissions associated with its production by the same amount. Therefore, it is expected that the future world production and use of GUL will significantly increase due to its ecological benefits.

While there are a number of studies on the hydration and strength characterization of concrete made with GUL cement (e.g. Li et al., 2017; Marzouki et al., 2013; Ramezanianpour and Hooton, 2013) and its response to durability issues such as sulfate attack (e.g. Ramezanianpour and Hooton, 2013), acidic attack (e.g. Amin and Bassuoni, 2018) and chloride ions penetration (e.g. Thomas et al., 2014), there has been dearth of information and field experience regarding the effect of GUL on the performance of concrete exposed to high concentration of de-icing salts. These types and concentrations of de-icing salts are comparable to that applied by different transportation agencies in North America (e.g. Policy on Snow Clearing and Ice Control, 2017; Minnesota Snow-Ice Control-Field Handbook for Snow Plow Operators, 2017) based local availability of the de-icing salt and effective freezing temperature in each region.

Recent studies by the Cementitious Materials research group at the University of Manitoba showed that GUL mixtures exhibited better resistance to freezing/thawing cycles combined with moderate concentration of de-icing salts (Ghazy and Bassuoni 2018). However, the adverse effects of high concentration of de-icing salts on concrete have been a key durability issue and a subject of extensive investigation, especially under continuous immersion at low temperatures (4–10°C) exposures (Ghazy and Bassuoni, 2017; Peterson et al., 2013). Generally, moderate concentration of de-icing salts can aggravate damage by increasing the level of moisture saturation and osmotic pressure in concrete, as well as due to the increased volume of salt crystallization during drying periods (Ghazy and Bassuoni 2018). However, damage can also be aggravated by interaction between concrete and de-icing chemicals, resulting in leaching and decomposition of cement hydration products when high concentration of de-icing salts are used (Ghazy and Bassuoni 2018; Ghazy and Bassuoni, 2017; Peterson et al., 2013).

OBJECTIVES

Given the current stipulations of specifications regarding the limits for GUL cement, the current study focus on substantiating the potential benefits of GUL cement, if any, in mitigating the adverse effects of high concentration of de-icing salts on concrete; hence, improve the current specifications and guidance for concrete exposed to extensive use of de-icing salts and consequently, the wider use of GUL cement in transportation infrastructure in North America.

EXPERIMENTAL PROGRAM

Materials and mixtures

General use limestone (GUL) cement with 11.3% limestone powder content, which meets the requirements of the CAN/CSA-A3001 standard (CSA 2019), was used as the main component of the binder. General Use (GU) cement, which represents typical concrete pavements cement in North America, was also used as a reference. In addition, Type F fly ash (designated as F) conforming to CSA A3001 (CSA, 2018) was used at dosages of 20% and 30% by the total binder content (i.e. 80 and 120 kg/m^3, respectively). The chemical and physical properties for GUL, GU, and fly ash are shown in **Table 1**. Six concrete mixtures were tested in this study; the total binder (GUL or GU cement and fly ash) content in all mixtures and the water-to-binder ratio (*w/b*) were kept constant at 400 kg/m^3 and 0.4, respectively. **Table 2** shows the mixture design proportions of the concrete tested in this study.

The target consistency of fresh concrete was achieved by high-range water reducing admixture (HRWRA) based on polycarboxylic acid and complying with ASTM C494 (ASTM, 2016c), Type F. This HRWRA was added at variable dosages (0 to 475 ml per 100 kg of the binder) to the mixtures in order to maintain a slump range of 50 to 100 mm. In addition, an air-entraining admixture was used to obtain a fresh air content of 6 ± 1%. The coarse aggregate used was mostly natural gravel (max. size of 9.5 mm) with a small proportion of carboniferous aggregate; its specific gravity and absorption were 2.65 and 2%, respectively. The fine aggregate was well-graded river sand with a specific gravity, absorption, and fineness modulus of 2.53, 1.5% and 2.9, respectively.

Constituent materials were mixed in a mechanical mixer and cast in prismatic molds (50×50×285 mm) to prepare triplicates for each mixture. Also, eight replicate cylinders (100×200 mm) were prepared in order to evaluate the compressive strength (**Table 2**) according to ASTM C39 (ASTM, 2016b), and the penetrability of chloride ions into concrete mixtures. The specimens were demoulded after 24 h and then cured for 28 days at standard conditions (22±2 °C and 98% RH) according to ASTM C192 (ASTM, 2016a). The curing period was kept constant to provide a uniform basis of comparison among all mixtures.

Table 1: Chemical composition and physical properties of GU cement, GUL and Fly Ash

	GU	GUL	Fly Ash
SiO_2 %	19.21	18.9	55.20
Al_2O_3 %	5.01	4.4	23.13
Fe_2O_3 %	2.33	3.2	3.62
CaO %	63.22	63.4	10.81
MgO %	3.31	0.7	1.11
SO_3 %	3.01	2.7	0.22
Na_2O_{eq} %	0.12	0.3	3.21
Specific Gravity	3.15	3.11	2.12
Mean Particle Size, µm	13.15	11.81	16.56
Blain Fineness, m^2/kg	390	454	290

Table 2: Proportions of mixtures per cubic meter of concrete

Mixture ID.	Cement (kg/m³)	Fly Ash (kg/m³)	Nanosilica (kg/m³)	Water[a] (kg/m³)	Coarse Aggregate (kg/m³)	Fine Aggregate (kg/m³)	28 day Compressive Strength (MPa)
GU group							
GU	400	--	--	160	1096	590	40 (0.3)[a]
GUF20	320	80	--	160	1077	580	38 (0.7)
GUF30	280	120	--	160	1068	575	35 (1.1)
GUL group							
GUL	400	--	--	160	1096	590	46 (0.4)
GULF20	320	80	--	160	1077	580	43 (1.2)
GULF30	280	120	--	160	1068	575	40 (0.8)

[a] The values between brackets in the last column are the standard errors

Exposures

To evaluate the durability of the tested mixtures to chloride-based de-icing salts, a continuous immersion exposure in which prismatic specimens were fully immersed in high concentration solutions of various de-icing salts at 5 °C up to 540 days was used. Sodium chloride (NaCl), dihydrate form of calcium chloride ($CaCl_2 \cdot 2H_2O$) and hexahydrate form of magnesium chloride ($MgCl_2 \cdot 6H_2O$) with purity of 99, 96 and 96%, respectively were used to prepare the solutions. **Table 3** shows the concentrations of the de-icing solutions used in the present study. Also, for better comparison between the de-icers used, an equal number of chloride ions (~160,000 ppm) among the three solutions was used to maintain similar ionic concentration of chloride ions in each solution. The solutions were renewed every four weeks to keep a continual supply of de-icing salts, thus providing aggravated damage conditions.

Table 3: Concentration of the de-icing salt solutions

Type of Salt	Salt Concentration Mass (%)	Chloride Concentration (mol/l)	Chloride Concentration[a] (ppm)
NaCl	23.3	4.52	160,071
$MgCl_2$	19.1	4.52	160,069
$CaCl_2$	21.9	4.51	160,067

[a] The ionic concentration of Cl⁻ ions in each solution was verified by ion chromatography (ASTM D 4327, 2011)

Tests

In order to evaluate the physical resistance, the rapid chloride permeability test (RCPT) was performed according to ASTM C 1202 (ASTM, 2012) on four specimens from each mixture. To minimize the effects of electrolysis bias and temperatures on the trends, the penetration depth of chloride ions/front into concrete, which better correlates to the physical characteristics of the pore structure, was determined (Bassuoni et al., 2006). Following the RCPT, the discs were axially split and sprayed with 0.1 M silver

nitrate solution which forms a white precipitate of silver chloride, to measure the average physical penetration depth of chloride ions.

Before exposure, the initial physico-mechanical properties of the intact specimens were measured. The initial mass and length (ASTM C 157 (ASTM, 2014a)) were measured before exposure. Specimens were removed from the solutions at specified time intervals (every 2 weeks), and the free expansion of prisms was immediately measured. Subsequently, debris, if any, were removed by a nylon brush, and the specimens were left to dry under 23±2°C and 50% RH for 30 min before visual inspection and measurement of mass. Relative to the initial values, the changes in mass and length versus time of exposure were calculated. The alteration of microstructure in deteriorating specimens was assessed by mineralogical and thermal analyses using X-ray diffraction (XRD, Cu-Kα) with a scanning rate of 0.5°/min and differential scanning calorimetry (DSC) with an incremental heating rate of 10°C/min on powder samples collected from the surface of specimens (within 10 mm). These specimens were first kept in a desiccator containing calcium sulfate for 5 days at 5±2°C. Subsequently, the powder was prepared from selected fracture pieces (not including large coarse aggregate) of specimens, which were pulverized to a fine powder passing through sieve #200 (75 µm).

RESULTS

Visual assessment and mass change

The condition of the specimens was regularly assessed visually (e.g. **Figure 1**). Also, the mass change of specimens with time was measured and summarized in **Table 4**. Up to 540 days of exposure, specimens from all mixtures subjected to continuous immersion in the NaCl solution experienced a steady mass gain (maximum of 2%) with time, without any distinctive visual features of damage. Comparatively, the reference specimens (GU and GUL) and specimens made with binary binders containing 20% fly ash (GUF20 and GULF20) exposed to $MgCl_2$ solution developed blisters at the surface, and the skin of the specimens started to peel off at approximately 90 to 180 days. With time, the deterioration was advancing with visible gel-like compound on/below the surface of the specimens accompanied by high intensity of cracks. Eventually, these specimens were softened, disintegrated, and showed notable swelling and mass loss (**Table 4**); thus, the physico-mechanical measurements were discontinued for these specimens. Similar features of damage were observed for both GU and GUL groups, except that the GUL group (GUL and GULF20) survived longer (**Table 4**) than the GU group (GU and GUF20). Specimens made with binary binders containing 30% fly ash (GUF30 and GULF30) were intact with no evidence of degradation up to the end of the exposure (540 days). $CaCl_2$ solution was the most aggressive solution as the rate of deterioration of specimens was very rapid. Micro-cracks along the edges of all specimens and clear separation of the surface layer from the rest of the specimen were the main features of damage at early stages of exposure. Additional cracks parallel to the edge of prisms progressively appeared and the deterioration of these specimens proceeded until complete disintegration due to macro-cracks with high magnitude of mass loss (**Table 4**), except specimens made with binary binders containing 30% fly ash and GUL cement (GULF30) were intact with no evidence of degradation up to the end of the exposure.
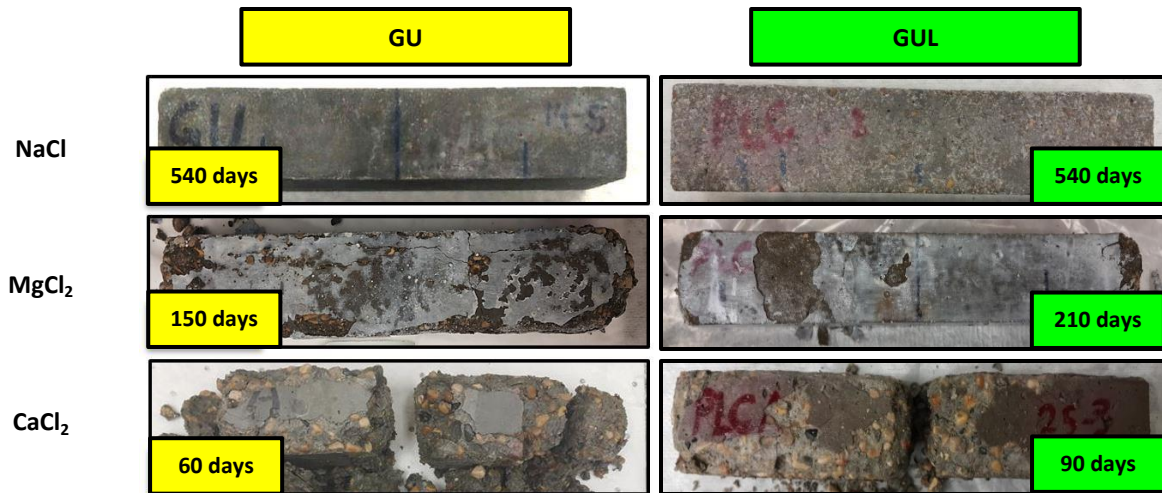
Figure 1: Exemplar visual features of damage for the reference specimens (GU and GUL) exposed to different de-icing salts.

Table 4: Results of mass change, expansion, and time of last measurement

Mixture ID.	NaCl			MgCl$_2$			CaCl$_2$		
	Mass change (%)	Expansion (%)	Time* (days)	Mass change (%)	Expansion (%)	Time* (days)	Mass change (%)	Expansion (%)	Time* (days)
GU group									
GU	1.0	0.02	540	- 20.6	1.56	150[†]	- 30.6	2.80	60[†]
GUF20	1.0	0.02	540	- 14.0	0.64	330[†]	- 25.5	1.07	180[†]
GUF30	2.0	0.03	540	1.0	0.05	540	- 17.8	0.70	360[†]
GUL group									
GUL	1.5	0.02	540	-16.3	1.11	210[†]	-21.4	2.14	90[†]
GULF20	1.0	0.02	540	-11.1	0.43	490[†]	-19.3	0.74	265[†]
GULF30	1.0	0.03	540	0.0	0.03	540	0.0	0.02	540

* Refers to the time of the last measurement.
[†] Specimens failed after this stage.

Expansion

Table 4 shows the total expansion of all specimens. The expansion was low (maximum of 0.03%) for all specimens immersed in the NaCl solution compared to other solutions. In contrast, the GU and GUL groups immersed in the MgCl$_2$ and CaCl$_2$ solutions showed high expansion before failure (**Table 4**), except binary binders containing 30% fly ash and GUL cement (GULF30). Generally, the GUL group exhibited notably low expansion compared to the GU group. For example, the control GUL specimens immersed in the MgCl$_2$ and CaCl$_2$ solutions yielded an expansion of 1.11% and 2.14% (reduction of 29%

and 24%, respectively) after 210 and 90 days (**Table 4**). Also, incorporating fly ash in the binder notably decreased the magnitude of the expansion irrespective of the type of solution. For example, the binary binders containing 20% fly ash (GUF20) immersed in the $MgCl_2$ and $CaCl_2$ solutions yielded an expansion of 0.64% and 1.07% (reduction of 59% and 63%, respectively) after 330 and 180 days (**Table 4**). The effect of fly ash was more pronounced in the GUF30 and GULF30 specimens. No expansion was recorded for both specimens immersed in the $MgCl_2$ solution and GULF30 specimens immersed in the $CaCl_2$ solution. Also, the GUF30 specimens immersed in the $CaCl_2$ solution yielded an expansion of 0.70% (reduction of 75%) after 360 days (**Table 4**).

RCPT

The physical resistance of all specimens after curing for 28 days was evaluated by the RCPT and the results are listed in **Table 5**. After completing the RCPT, the physical penetration depth of chloride front was measured for concrete specimens as indicated by the whitish precipitate (**Figure 2**). Also, the non-steady-state migration coefficient was calculated based on the penetration depth, geometry of specimen, applied voltage, temperature of the anolyte solution and test duration, according to NT BUILD 492 (2011), to account for the heat (Joule) effect and different testing durations, if any, on ionic mobility within specimens.

The control GUL specimens showed about 26% reduction in penetration depth relative to the control GU specimens. This might be due to the higher fineness of the PLC (460 m^2/kg) in comparison with the GU (390 m^2/kg), due to intergrinding of limestone powder with clinker, which can improve the hydration process and microstructural evolution of concrete (Ramezanianpour and Hooton, 2014). In addition, the filler effect resulting from the continuous particle size distribution of GUL may yield better particle packing in the matrix (Ghiasvand et al., 2015). However, this trend was invalid or diminished for the other mixtures due to the predominant effect of fly ash (e.g. compare mixes GULF20 and GULF30 with, respectively, GUF20 and GUF30). This trend highlights the role of fly ash in refining and densifying the pore structure of the matrix and thus reducing its penetrability.

Table 5: RCPT Results

Mixture ID.	Charges Passed (coulombs)	Chloride Ions Penetrability Class, ASTM C1202	Average Penetration Depth (mm)	Migration Coefficient, $\times 10^{-12}$ (m^2/s)
GU group				
GU	2248	Moderate	17.6 [0.94][a]	17.67
GUF20	1527	Low	12.8 [0.64]	10.16
GUF30	1253	Low	10.1 [0.57]	8.16
GUL group				
GUL	1867	Low	13.1 [1.07]	12.93
GUL20	1370	Low	11.4 [1.14]	9.81
GULF30	917	Very Low	9.4 [0.96]	8.01

[a] Standard error is shown between brackets
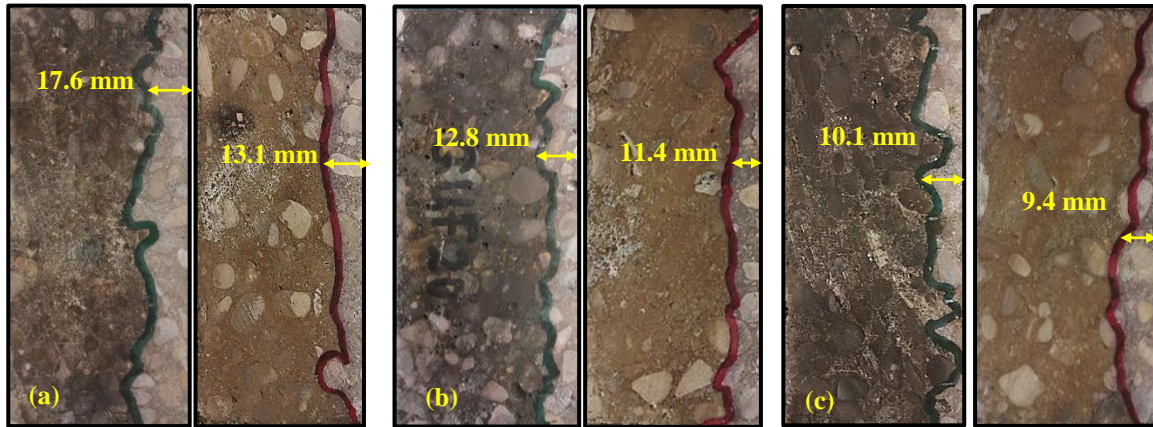
Figure 2: Whitish precipitates showing the average penetration depth of chloride ions in specimens (GU left and GUL right): (a) control mixture, (b) mixtures with 20% fly ash, and (c) mixtures with 30% fly ash.

DISCUSSION

### Effect of type of solution

The mechanisms of damage were similar for both GU and GUL group within each salt solution. Thus, in this section, the GUL specimens are presented in order to demonstrate these mechanisms for each salt solution. Subsequently, the effect of type of cement and fly ash on the mechanisms of damage will be discussed.

No signs of deterioration were observed for all specimens immersed in NaCl solution. Portlandite, calcite, quartz and dolomite were shown in the XRD similar for the corresponding specimens immersed in deionized water, except Friedel's salt and ettringite peaks were observed (**Figure 3**). Binding chloride ions by aluminate phases to form chloroaluminate phases such as Friedel's salt may not be detrimental to the integrity of the hydrated cement paste as no marked symptoms of expansion, cracking, spalling and softening were observed for the specimens. The peaks of dolomite and calcite might have occurred because the coarse aggregate contained a fraction (about 10 to 15%) of carboniferous aggregate, while the sources of quartz in the diffractograms originated from the siliceous coarse aggregate and sand in all mixtures.

For MgCl$_2$ solution, the XRD patterns showed dominant phases of magnesium oxychloride (in various forms; 3- and 5-form), brucite, gypsum, quartz, dolomite and calcite (**Figure 3**). This might be attributed to the saturation of the pore fluid with respect to magnesium, calcium, chloride, and hydroxyl ions. The major cause of deterioration by MgCl$_2$ is likely the chemical activity resulting in formation of relatively expansive (magnesium oxychloride) and softening (gypsum) phases.

Calcium oxychloride, Friedel's salt and ettringite were the main reaction phases detected in the XRD patterns (**Figure 3**). Also, portlandite diminished due to its consumption in the formation of calcium oxychloride. Formation of calcium oxychloride was accompanied by significant expansion and cracking, which led to the notable disintegration of specimens, as shown earlier in the Results Section.
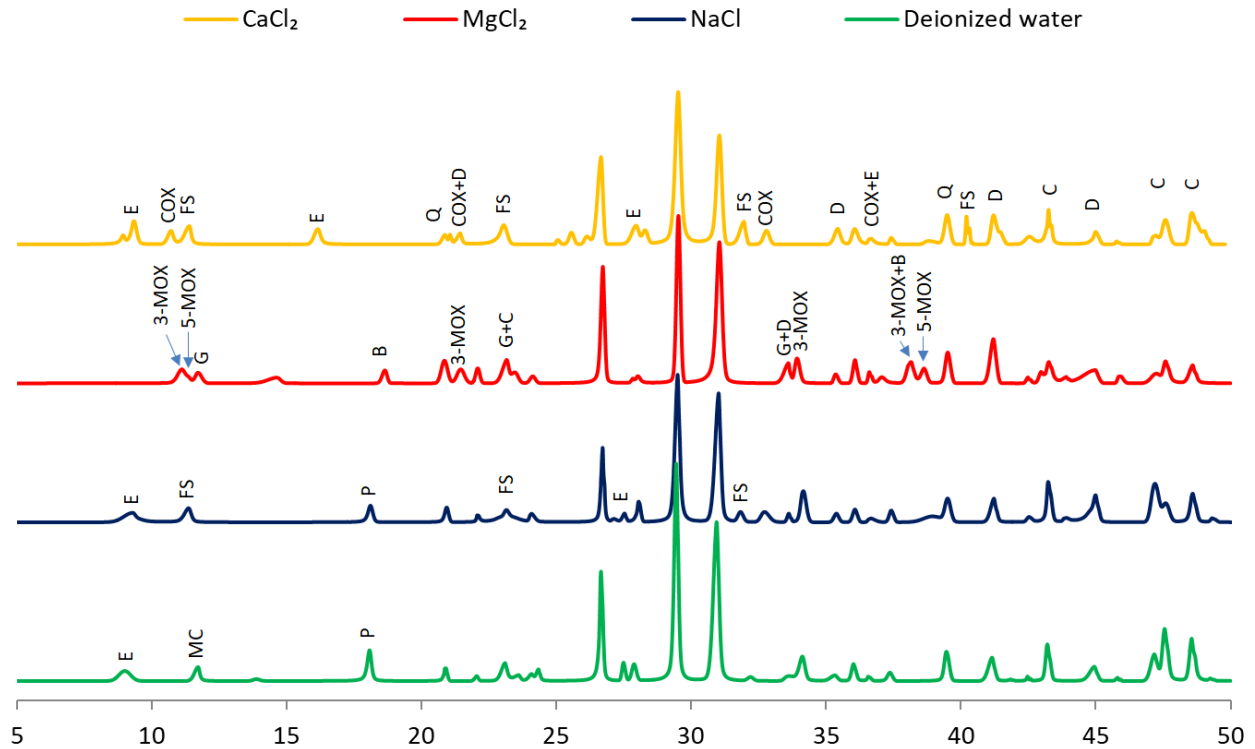
Figure 3: XRD patterns of the GUL specimens continuously immersed in different solutions at the time of failure listed in Table 4. *(Note 2: E = Ettringite, P = Portlandite, FS = Friedel's salt, COX = Calcium oxychloride, 3-MOX = 3-Form Magnesium oxychloride, 5-MOX = 5-Form Magnesium oxychloride, B = Brucite, D = Dolomite, C = Calcite, Q = Quartz, G = Gypsum).*

Effect of type of cement

Generally, the GUL group performed better (less mass loss) and survived longer (high retention of stiffness) than the GU group as shown earlier in the Results Section, irrespective of the type of the solution. This improvement can be ascribed to the synergistic physical and chemical actions of the limestone component in the GUL cement.

Physically, the control GUL specimens showed about 26% reduction in the penetration depth relative to the control GU specimens. Intergrinding limestone powder with clinker during production led to higher fineness of the GUL cement (460 m^2/kg) in comparison to the GU cement (390 m^2/kg), which may improve the hydration process and microstructural evolution of concrete. In addition, the filler effect resulting from the continuous particle size distribution of GUL may yield better particle packing in the matrix (Marzouki et al. 2013). Accordingly, GUL mixtures had reduced ingress of salt solutions and consequently better physical resistance to ingress of de-icing salts.

Chemically, the limestone component in GUL specimens also changed the hydration pattern of the binder as shown by the XRD for the reference sample in **Figure 4**. Carboaluminate appeared as a distinctive reaction product between limestone powder and various aluminate compounds (e.g.

hydroxy-AFm and monosulfate). The formation of carboaluminate-type compounds in portland-limestone cements was also observed in previous studies. The ability of carboaluminate hydrates to bind chloride was also reported to be significantly less than other AFm compounds (e.g. monosulfate) (Ipavec et al. 2013); therefore, lower intensities of Friedel's salt and consequently, formation of the complex salts (oxychlorides). On the other hand, the lower clinker component (due to dilution by 12% interground limestone) in the GUL cement reduced the initial portlandite (at 28 days) in these mixtures; subsequently, the potential for the chemical activity. This was corroborated herein by the lower intensities of portlandite peaks in the XRD pattern. This was also substantiated by the DSC results (17% reduction of the initial portlandite content compared to GU mixture, **Table 5**). Moreover, the GUL mixtures had lower C_3A content relative to the GU mixtures resulting in slower chemical activity (incipient formation of Friedel's salt). These physical and chemical effects of limestone explain the improvement in the resistance of GUL mixtures to degradation.
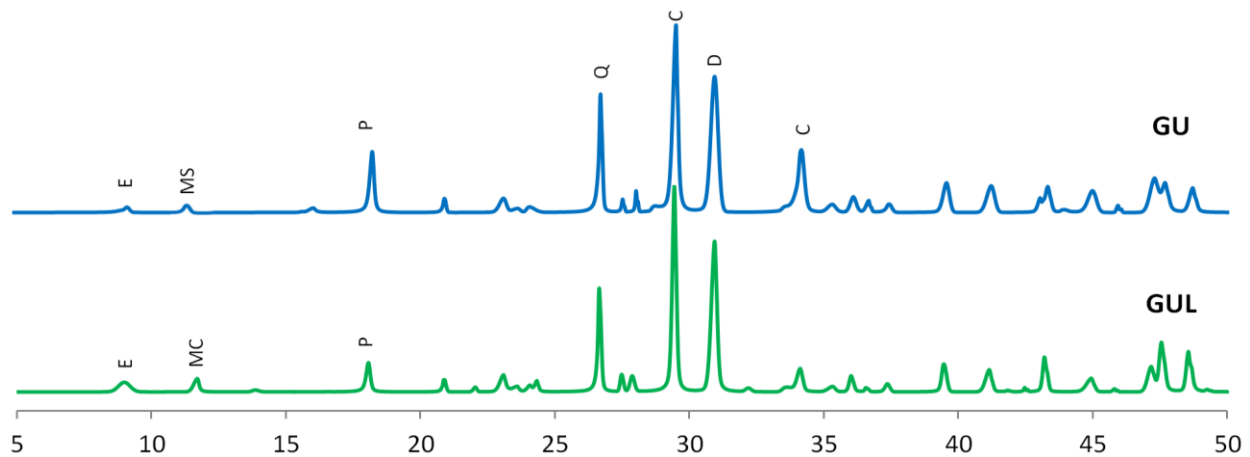
Figure 4: XRD analysis of GU and GUL specimens before exposure. (*Note: E=Ettringite, P=Portlandite, MS=Monosulfate, MC=Monocarboaluminate, Q=Quartz, D=Dolomite, C=Calcite*)

Effects of Fly Ash

Compared to the single binder (GU and GUL) mixtures, the incorporation of fly ash in binary binders reduced the penetrability of concrete. For instance, adding 20 and 30 % fly ash in binary binders (GULF20 and GULF30) led to approximately 13% and 29% reduction in the penetration depth of specimens compared to that of the corresponding specimens prepared with the GUL cement only, which was 12.93 mm (**Table 5**). The reduction of the penetration depth/migration coefficient may be attributed to the reduction of the effective porosity; thus, reducing the penetrability of the matrix (increased physical resistance). In addition, the initial portlandite content in these specimens decreased with increasing the dosage of fly ash in the binders (**Table 5**) owing to the dilution of the cement component, consequently limiting the chemical activity. Hence, fly ash mixtures performed better and/or survived longer than the reference GU or GUL specimens, especially the mixture containing 30% fly ah, as shown earlier in the Results section.

The DSC results showed that there was no efficient later-age pozzolanic activity of Type F fly ash in the binary specimens as indicated by the presence of high portlandite contents at the end of the exposure (maximum consumption of 7% after 540 days, **Table 5**). This implies that the long-term activity of fly ash was hindered at this low temperature (5°C), especially that these specimens were initially cured for 28 days. Hence, the binary fly ash specimens generally failed (but after the GU specimens with higher initial portlandite contents and penetrability) under this exposure before 540 days, especially with the aggressive types of salt solutions (**Table 4**). Perhaps, if the binary specimens comprising 20 and 30% fly ash were initially cured for longer periods (56 days or more) before exposure, the effect of fly ash might have been more improved. The effect of fly ash was magnified in the GUL group owing to the improvement effect of the limestone component in cement, as discussed earlier.

Table 5: Enthalpies (J/g) of portlandite in the cementitious matrix

Mixture ID.	After 28 days in the curing chamber	After 540 days immersed in deionized water	After 540 days or at the failure point* immersed in the de-icing salts		
			NaCl	MgCl$_2$	CaCl$_2$
GU group					
GU	63.6	62.1	42.3	0.0*	0.0*
GUF20	56.8	50.4	38.9	0.0*	0.0*
GUF30	45.8	39.7	31.8	22.9	0.0*
GUL group					
GUL	53.6	48.3	37.4	0.0*	0.0*
GULF20	48.3	42.7	33.9	0.0*	0.0*
GULF30	38.8	32.3	26.1	20.7	21.2

CONCLUSIONS

Based on the exposure procedure, test period, type of salt, and mixture design variables adopted in this study, the following conclusions can be drawn:

- NaCl is not an aggressive salt with respect to degradation of concrete as no signs of deterioration were observed. In contrast, MgCl$_2$, and CaCl$_2$ are aggressive as they enter into chemical reactions with cement-based materials, forming complex salts (oxychloride, Friedel's salt, ettringite, and gypsum, depending on the type of solution).
- GUL mixtures generally had better resistance to degradation by deicing salts due to synergistic physical and chemical actions of the limestone component in the binder.
- The results show that the resistance of concrete exposed to high concentrations of de-icing salts is a function of physical penetrability, amount of C$_3$A in cement and content of portlandite available for chemical reactions in the hydrated paste.
- Incorporation of 30% fly ash in concrete improved its resistance to degradation by de-icing salts due to reduced solution uptake and amount of portlandite.

The overall results from this study implicate that the restrictive limits on GUL cement and fly ash dosage in concrete exposed to high concentration of de-icing salts, stipulated in most North

American guides and specifications for concrete, may produce concrete less durable than alternative noncompliant mixtures with GUL cement and higher fly ash dosages. Thus, concerted efforts are needed to improve and update current guides and specifications for durability of concrete, especially with the intensive winter maintenance practices adopted by transportation agencies to cope with climatic changes.

REFERENCES

Amin, M., and Bassuoni, M.T. (2018) "Response of concrete with blended binders and nanoparticles to sulfuric acid attack" *Mag. Concr. Res*., 70(12): 617–632

ASTM (American Society for Testing and Materials). (2012). "Standard test method for compressive strength of cylindrical concrete specimens." *ASTM C39-12*, West Conshohocken, PA, USA.

ASTM (American Society for Testing and Materials). (2013). "Standard specification for chemical admixtures for concrete." *ASTM C494/C494M-13*, West Conshohocken, PA, USA.

ASTM (American Society for Testing and Materials). (2014). "Standard Test Method for Length Change of Hardened Hydraulic-Cement Mortar and Concrete." *ASTM C157-14*, West Conshohocken, PA, USA.

ASTM (American Society for Testing and Materials). (2016). "Standard practice for making and curing concrete test specimens in the laboratory." *ASTM C192-16*, West Conshohocken, PA, USA.

ASTM (American Society of Testing Materials). (2012). "Standard test method for electrical indication of concrete's ability to resist chloride ion penetration." *ASTM C1202-12*, West Conshohocken, PA, USA.

Bassuoni, M.T. and Nehdi, M.L. (2006), "Enhancing the reliability of evaluating chloride ingress in concrete using the ASTM C 1202 rapid chloride penetrability test", *J. ASTM Int.*, **3**(3), 13p.

City of Winnipeg, Policy on Snow Clearing and Ice Control, http://www.winnipeg.ca, (2011) (August 10, 2017).

CSA (Canadian Standards Association). (2019). "Cementitious materials for use in concrete." *CSA-A3001-13*. Canadian Standards Association, Mississauga, ON, Canada.

Ghazy, A. and Bassuoni, M.T. (2017), "Resistance of concrete to different exposures with chloride-based salts", *Cem. Concr. Res.*, **101**, 144-158.

Ghazy, A., Bassuoni, M.T. and Islam, A.K.M. R. (2018), "Response of concrete with blended binders and nanosilica to freezing-thawing cycles and different concentrations of de-icing salts", *J. Mater. Civ. Eng.*, 30(9): 04018214.

Ghiasvand, E., Ramezanianpour, A.A., and Ramezanianpour, A.M. (2015) "Influence of grinding method and particle size distribution on the properties of Portland-limestone cements" Materials and Structures 48(5): 1273–1283.

Ipavec, A., Vuk, T., Gabrovšek, R., Kaučič, V. (2013). "Chloride binding into hydrated blended cements: the influence of limestone and alkalinity." *Cem. Concr. Res.,* 48, 74-85.

Li LG, Chen JJ and Kwan AK (2017) Roles of packing density and water film thickness in strength and durability of limestone fines concrete. Proc. ICE – Mag. Concr. Res. 69(12): 595–605.

Marzouki, A., Lecomte, A., Beddey, A., Diliberto, C., Ouezdou, M.B. (2013). "The effects of grinding on the properties of Portland-limestone cement." *Constr. Build. Mater.,* 48, 1145-1155.

Minnesota Snow and Ice Control. (2012). "Field Handbook for Snowplow Operators." http://www.mnltap.umn.edu/ (May 1, 2017).

NORDTEST. (1999). "Chloride migration coefficient from non-steady-state migration experiments." NT BUILD 492, Finland.

Peterson, K., Betancourt, G., Sutter, L., Hooton, R.D., Johnston, D. (2013). "Observations of chloride ingress and calcium oxychloride formation in laboratory concrete and mortar at 5 °C." *Cem. Concr. Res.,* 45, 79-90.

Ramezanianpour, A.M. and Hooton, R.D. (2014) "A study on hydration, compressive strength, and porosity of Portland- limestone cement mixes containing SCMs" Cement & Concrete Composites 51: 1–13.

Ramezanianpour, A.M., Hooton, R.D. (2013). "Sulfate resistance of Portland-limestone cements in combination with supplementary cementitious materials." *Mater. Struct.,* 46(7), 1061-1073.

Thomas, M.D.A., Cail, K., Blair, B., Delagrave, A., Masson, P., Kazanis, K. (2014). "Use of Low-CO_2 Portland Limestone Cement for Pavement Construction in Canada." *Inter. J. Pave. Res. Tech.,* 3(5), 228-233.

DEDICATION

We would like to pay our gratitude and respects to the late Mr. Rod Hamilton, City of Winnipeg (COW), who helped in initiating and coordinating this project between COW and University of Manitoba. Mr. Hamilton passed away in April 2020. He played an instrumental role in the development of Public Works asset management and pavement research practices. In 2016, Mr. Hamilton was promoted to the Manager of Asset Management, COW where he finished his career.